Organic &
Biomolecular
Chemistry

Cite this: *Org. Biomol. Chem.*, 2011, **9**, 6396

www.rsc.org/obc

**PAPER**

# Kinetic control of the direction of inclusion of nitroxide radicals into cyclodextrins†

**Paola Franchi, Costanza Casati, Elisabetta Mezzina and Marco Lucarini***

***Received 18th April 2011, Accepted 17th June 2011***
**DOI: 10.1039/c1ob05618b**

*N*-benzyl-*tert*-butyl nitroxide derivatives substituted at the aromatic ring form host–guest inclusion complexes with β-and γ-cyclodextrin. They were employed as probes to assess substituent effects on the geometry of the complex and on the kinetics of this complexation by combining EPR and $^1$H NMR data.

## Introduction

Control of the direction of incorporation of a guest into a host and the relative molecular motion that takes place within the complexes is of importance for the construction of molecular machines.[1–3] Pseudorotaxanes and rotaxanes are considered to be a typical prototype of molecular machines bearing a rotor and an axle in the molecule.[4] When nonsymmetric macrocyclic derivatives like calixarenes[5] and cyclodextrins (CDs)[6] are used as three-dimensional rotor components, a significant increase in structural complexity is possible because randomly oriented structures deriving from the threading of suitable axles from the two different rims of the host could be formed.

Harada and co-workers were able to report in detail the face-selective threading of a CD molecule onto an axle compound with one or two station moieties to give kinetically preferred [2]- and [3]pseudorotaxanes.[7] In particular, a methyl group at the 2-position of a pyridinium group on the end cap of an axle molecule consisting of polymethylene units was found to control the rates of threading of α-CD. This was the first observation that the terminal group of an axle molecule controls kinetically the direction of faces of plural ring components in the rotaxane structure. These results represented a significant step forward for the construction of instructed chemical systems in which not only the equilibrium states but also the dynamic behaviour could be carefully controlled.

*N*-Benzyl-*tert*-butyl nitroxide (BTBN) has been largely used in our previous work as a paramagnetic guest species for studying cyclodextrin host systems.[8–9] Due to the sensitivity of its spectroscopic parameters (in water: $a$(N) = 16.69 G, $a(2H_\beta)$ = 10.57 G, $g$ = 2.0056)[8] to the polarity of the environment, and to conformational changes, after inclusion, BTBN shows large variations of the hyperfine splitting constants at both nitrogen and benzylic protons: $a$(N) = 15.74 G, $a(2H_\beta)$ = 7.88 G, $g$ = 2.0058. Thus, in the presence of a suitable host system,[10] EPR spectra of this radical show signals clearly different for the free and included species, and their ratio provides the value of the equilibrium constant for the formation of the inclusion complex. In addition, because the lifetimes of the two species are comparable to the time scale of EPR spectroscopy, as suggested by the strong dependence on the temperature of the spectral line width, this technique permits us to obtain information on the kinetics of association and dissociation of the inclusion complex.[8]

Kotake and Janzen have investigated in the late eighties the thermodynamic factors governing the competitive inclusion of two different groups inside a CD cavity by using spin probes and EPR spectroscopy.[11] However, to obtain pseudorotaxanes and rotaxanes characterised by a univocal and programmable relative orientation of their components, it is important to gain a deep understanding not only of the structural and thermodynamic factors governing the inclusion processes but also of the kinetic aspects of complexation. For this reason we decided to employ different nitroxides deriving from BTBN (**1b–6b**, Scheme 1) having one or two substituents on the aromatic ring and EPR spectroscopy to obtain accurate rate constants for the formation/dissociation of complexes between β-CD and γ-CD. The selected nitroxides were chosen because (*i*) they all maintain the favorable EPR features found in the related benzyl *tert*-butyl nitroxide, (*ii*) they can be obtained easily by oxidation of the corresponding amine precursors **1a–6a,** (*iii*) the presence of the aromatic substituents governs both the degree and the geometry of complex formation of CD with the guest molecules.

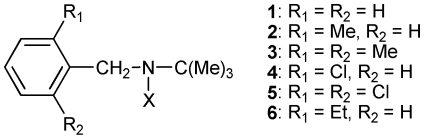


**1**: $R_1 = R_2 = H$
**2**: $R_1$ = Me, $R_2$ = H
**3**: $R_1 = R_2$ = Me
**4**: $R_1$ = Cl, $R_2$ = H
**5**: $R_1 = R_2$ = Cl
**6**: $R_1$ = Et, $R_2$ = H

**1a** - **6a**: X= H
**1b** - **6b**: X=O•

**Scheme 1**

*Department of Organic Chemistry "A. Mangini", University of Bologna, Via San Giacomo 11, I-40126 Bologna, Italy. E-mail: marco.lucarini@unibo.it*

† Electronic supplementary information (ESI) available: General notes and 2D-ROESY spectra of host–guest complexes. See DOI: 10.1039/c1ob05618b

To fully clarify the relationship between the geometry of the CD assemblies and the complexation kinetics, EPR data were correlated with $^1H$–$^1H$ NOE measurements carried out on the complexes between CD's and the structurally related amine precursors **1a–6a**.

## Results and discussion

### EPR measurements

The radical probes we used in this study belong to a family of *ortho*-substituted benzyl-*tert*-butyl nitroxides (**1b–6b**, Scheme 1). They were generated directly inside an EPR tube by oxidizing the parent amine (0.5 mM) with the magnesium salt of monoperoxyphthalic acid (0.5 mM) in the presence of variable amounts of CD. The amine precursors were prepared by reacting *tert*-butylamine with the appropriately substituted benzaldehyde followed by reduction with $NaBH_4$ (see Experimental section).

Good EPR spectra of nitroxides **1b–6b** in water were obtained in all cases by oxidation of the corresponding amines both at 298 K and 328 K. As an example, in Fig. 1a it is reported the spectrum obtained by oxidizing amine **4a** in water at 328 K. All spectra were easily interpreted on the basis of the coupling of the unpaired electron with nitrogen, and with the two benzylic protons (see Table 1). When the EPR spectra of radicals **1b–6b** were recorded in the presence of CD, additional signals were observed assigned to the radical included in the cavity of cyclodextrin, in equilibrium with the free nitroxide.‡ As an example, Fig. 1b reports the spectrum of **4b** recorded in the presence of 10 mM β-CD. By increasing the absolute concentration of CD, it was possible to increase the amount of the included radical (see Fig. 1c) which in most cases became the dominant species. In Table 1 are reported the spectroscopic parameters for the included nitroxides.

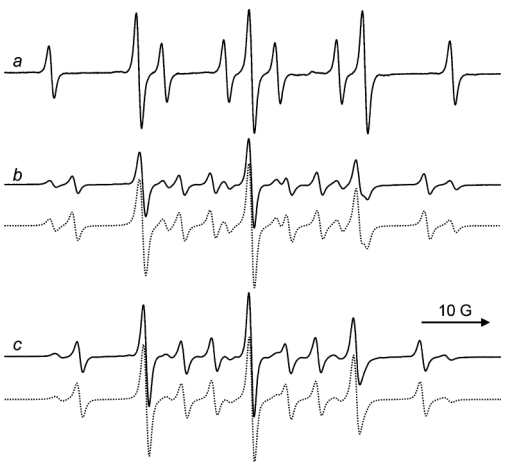


**Fig. 1** EPR spectra at 328 K of nitroxide **4b** in water (a) and in the presence of β-CD 10 mM (b) and 17 mM (c). Theoretical simulations are reported as dotted lines.

‡ Recently, the first example of inclusion complexes between a CD derivative and aromatic guests possessing no charge and no acidic hydrogen in nonpolar solvents has been reported (see reference 13). In particular, it was shown that chlorinated benzenes can be included inside the cavity of heptakis(6-*O*-*tert*-butyldimethylsilyl)-*β*-cyclodextrin (TBDMS-β-CD) in nonpolar solvents like benzene or cyclohexane. Based on this, we checked by EPR if also chlorinated nitroxides such as **4b**, **5b** and (2,4,5-trichloro)-1-benzyl-*tert*-butyl nitroxide could form inclusion complexes with TBDMS-β-CD. Unfortunately, we did not have any evidence by EPR of the formation of inclusion complexes both in benzene and cyclohexane. This result suggests that the behaviour observed by Kida *et al.* cannot be generalised to chlorinated benzenes having other substituents.

**Table 1** EPR parameters[a] of nitroxides **1b–6b** (1G = 0.1 mT) and rate constants[b] for their complexation by β-cyclodextrin in water at 328 K

| Nitroxide | $R_1$, $R_2$ | $a(2H_\beta)$ | $a(N)$ | $k_{ass}/M^{-1}\,s^{-1}$ | $k_{diss}/s^{-1}$ | $K_{Eq}/M^{-1}$ |
|---|---|---|---|---|---|---|
| **1b** | H, H | 10.19 | 16.56 | $1.5\times10^9$ | $2.5\times10^6$ | 600 |
| | | **7.58** | **15.64** | | | |
| **2b** | Me, H | 13.01 | 16.87 | $8.6\times10^8$ | $3.8\times10^6$ | 226 |
| | | **10.81** | **16.10** | | | |
| **3b** | Me, Me | 17.93 | 17.37 | $4.9\times10^8$ | $3.5\times10^6$ | 140 |
| | | **16.71** | **16.61** | | | |
| **4b** | Cl, H | 13.03 | 16.83 | $8.7\times10^8$ | $2.4\times10^6$ | 362 |
| | | **10.24** | **15.96** | | | |
| **5b** | Cl, Cl | 17.10 | 17.35 | $6.2\times10^8$ | $2.3\times10^6$ | 269 |
| | | **15.63** | **16.79** | | | |
| **6b** | Et, H | 12.88 | 16.88 | $8.2\times10^8$ | $3.8\times10^6$ | 216 |
| | | **10.63** | **16.10** | | | |

[a] The values given in bold type refer to the radical included in the β-CD cavity. [b] Estimated uncertainty *ca.* 10%.

The equilibrium constants ($K_{Eq}$) for the complex formation between nitroxides **1b–6b** and the investigated CD were determined from the values of the rate constants for association ($k_{ass}$) and dissociation ($k_{diss}$) of the complex, obtained from the simulation of the exchange-broadened EPR spectra, by using well-established procedures based on the density matrix theory[8] and assuming a two-jump model as illustrated in Scheme 2.

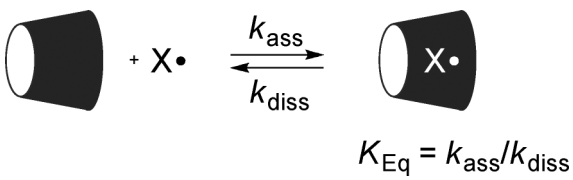


**Scheme 2**

### EPR kinetic data

As expected, the kinetic data in Table 1 show that the rate constants for the inclusion of the guest radical by β-CD, $k_{ass}$, depend both on the nature and the number of the substituents at the 2 and 6 positions of the aromatic ring. With the mono- (**2b**, **4b** and **6b**) and di-substituted derivatives (**3b** and **5b**), a reduction of *ca.* two and three times, respectively, in the value of the association rate, $k_{ass}$, is observed compared to the unsubstituted BTBN.

The relatively small variation of $k_{ass}$ observed is similar to that reported by Nau and coworkers during the investigation on the substituent effects on host–guest complexation of bicyclic azoalkanes by β-CD.[12]

The smaller values of the association observed in the presence of substituted radicals indicate the presence of a larger steric hindrance between the aromatic substituents and the rim of the β-CD. This hypothesis is corroborated by the observation of less marked differences in the values of $k_{ass}$ with γ-CD. Actually, in the presence of the larger member of the cyclodextrin family, where steric effects on the inclusion process are expected to be less

**Table 2** EPR parameters[a] of nitroxides **1b–6b** (1G = 0.1 mT) and rate constants[b] for their complexation by γ-cyclodextrin in water at 295 K

| Nitroxide | $R_1$, $R_2$ | $a(2H_\beta)$ | $a(N)$ | $k_{ass}/M^{-1}\ s^{-1}$ | $k_{diss}/s^{-1}$ | $K_{Eq}/M^{-1}$ |
|---|---|---|---|---|---|---|
| **1b** | H, H | 10.63 | 16.71 | $3.8 \times 10^8$ | $7.6 \times 10^6$ | 50.7 |
| | | **8.02** | **15.97** | | | |
| **2b** | Me, H | 13.63 | 16.97 | $2.7 \times 10^8$ | $5.3 \times 10^6$ | 50.9 |
| | | **10.91** | **16.24** | | | |
| **3b** | Me, Me | 18.37 | 17.47 | $3.1 \times 10^8$ | $7.0 \times 10^6$ | 44.2 |
| | | **16.41** | **16.84** | | | |
| **4b** | Cl, H | 13.75 | 16.98 | $2.9 \times 10^8$ | $4.1 \times 10^6$ | 70.7 |
| | | **10.68** | **16.21** | | | |
| **5b** | Cl, Cl | 17.52 | 17.50 | $2.7 \times 10^8$ | $3.2 \times 10^6$ | 84.4 |
| | | **15.66** | **16.80** | | | |
| **6b** | Et, H | 13.43 | 17.00 | $3.0 \times 10^8$ | $3.0 \times 10^6$ | 100 |
| | | **10.90** | **16.39** | | | |

[a] The values given in bold type refer to the radical included in the γ-CD cavity. [b] Estimated uncertainty *ca.* 10%.

important, rate constants for the association $k_{ass}$ are very similar for all the investigated nitroxides (see Table 2).

The dissociation rate constants ($k_{diss}$) define the lifetimes of the guests in the CD cavity and cannot be easily related to the bulkiness of the aromatic substituents. While with alkyl groups the larger values of $k_{diss}$ are consistent with the larger steric hindrance between the guest and the internal cavity of β-CD, with both chlorine substituted nitroxides **4b** and **5b**, $k_{diss}$ is very similar to the value measured for the unsubstituted derivative. In this case the increased steric hindrance of the guest due to the presence of a second chlorine atom is balanced by the increased dipole–dipole interactions between the host cavity and the guest molecule which are known to be important in stabilizing the complex with guests containing chlorine atoms.[12,13]

This interpretation was confirmed by measuring $k_{diss}$, in the presence of γ-CD. In this case steric effects are less important and $k_{diss}$ for **4b** and **5b** are smaller with respect to the value measured with BTBN due to the favourable dipole–dipole interaction present in the former cases.

### Geometry of the complexes

In principle, two modes of accommodation in the larger rim are possible with nitroxides **1b–6b**: either from the *tert*-butyl side or from the phenyl side. By using NMR, we were able in the past to demonstrate that in BTBN the inclusion is occurring from the benzyl side.[14]

For the substituted probes **2b–6b**, however, the increased bulkiness of the benzyl substituents could result in a change in the geometry of the complex. In order to get insight into the geometry of the inclusion complexes in liquid phase between the investigated paramagnetic compounds and cyclodextrins, we decided to repeat $^1$H NMR experiments with the diamagnetic related precursors of the nitroxides, *i.e.* amines **1a–3a** and **6a**, in the absence and in the presence of β-CD and γ-CD. The choice of amine precursor was determined by the difficulties associated with the characterization of paramagnetic species through NMR.

The spectra were measured for $D_2O$ samples containing 5% $CD_3OD$ to ensure complete dissolution of *N*-benzyl-*tert*-butyl amine (BTBA) derivatives. 2D ROESY experiments were carried out in solutions of amines containing from 0.2 to equimolar amounts of β-CD and γ-CD, with mixing times 300 ms. Analysis of ROESY spectra gave a clear indication on the inclusion direction of the guest and the results are discussed below (see also Scheme 3).

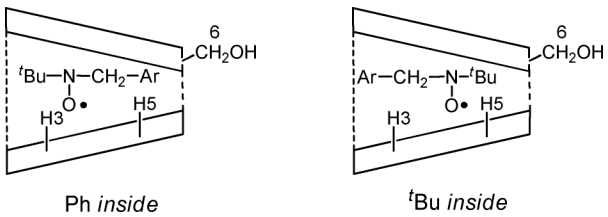


**Scheme 3**

The ROESY spectrum of non-substituted benzyl *tert*-butylamine **1a** in the presence of β-CD shows significant interactions of the *tert*-butyl protons of the guest molecule with the inner H3 (strong) and H5 (medium) cyclodextrin protons. The spectrum shows also cross-peaks correlating aromatic protons only with overlapped H5/H6 (medium) protons located at the smaller edge of the macrocyclic host, while correlations of the phenyl peaks with the CD inner H3 signal were never detected (see the ESI†).

Concerning the position of the benzyl protons, the interpretation of the NMR spectra of the inclusion complexes was difficult to achieve, due to its close chemical shift value with the cyclodextrin H3–H6 proton signals (3.70–4.00 ppm). In this case the detection of distinct cross-peaks was difficult due to overlapping and the same behavior was observed for all the amines analyzed in this study.

Anyway, these results suggest that inclusion of **1a** into the CD cavity occurs from the phenyl portion of BTBA which is located close to the primary (*i.e.* the smaller) CD rim, and the *tert*-butyl group of the guest is accommodated near the secondary (*i.e.* the larger) side of the host. This geometry agrees well with previous results obtained by us in a study of the solution structure of the complex of the same amine with 2,6-*O*-dimethylated β-CD.[14]

The opposite conclusions were achieved when analyzing the complex geometry of **1a** included in the larger γ-cyclodextrin cavity. In this case, $^1$H–$^1$H ROESY interactions of aromatic protons with H3 are the only connections detected, while *tert*-butyl protons are deeply included in the macrocycle revealing not only cross-peaks with inner H3 and H5, but also a weak interaction with H6 protons surrounding the minor rim of the host (see the ESI† and Scheme 3). From these experimental data we deduced that the phenyl ring of the amine is near the secondary edge of γ-CD in a reverse geometry with respect to the smaller β-CD.

ROESY spectra were also recorded for solutions containing amine **2a** and β-CD in 0.2 : 1.0 host : guest stoichiometric ratio. Cross-peaks were detected between *tert*-butyl protons and the H3, H5, and H6 protons of CD (see Fig. 2). In this spectrum the splitting of CD H5 and H6 signals allowed us to observe distinct cross peaks for each proton which were stronger for H5 than for minor rim H6, and an intense interaction was recorded also with the inner H3 of the host (square in plot *b*, Fig. 2).

More interestingly, the aromatic protons of amine **2a** displayed an interaction only with the H3 signal (plot *a*, Fig. 2) in contrast to what was observed in the case of **1a**. Finally, cross peaks between the signal of the *ortho*-methyl substituent and CD H5 and H6 protons were not observed while a weak interaction with H3 was detected.

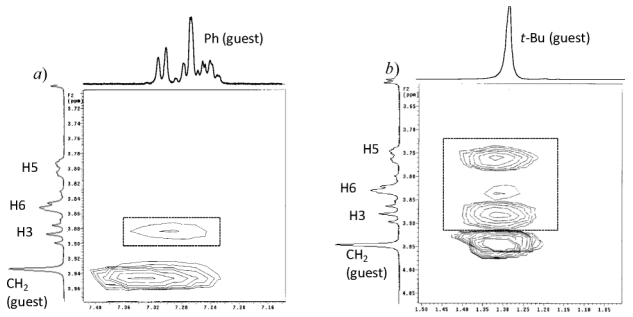


**Fig. 2** Portion of the ROESY spectra of a 0.5 mM solution of **2a** (right, X range from 1.00 to 1.50 ppm, Y range from 3.60 to 4.07 ppm; left, X range from 7.14 to 7.41 ppm, Y range from 3.70 to 3.97 ppm) containing 0.1 mM β-CD in $D_2O$ at 298 K. The dotted line square evidences in the plot *a* the cross peak connecting the phenyl ring protons of **2a** with H3 CD protons only, which was not observed with H5 and H6. The square in the plot *b* highlights the deep inclusion of the *tert*-butyl portion of the amine into the CD.

The analysis of these results reveals an opposite direction of inclusion of the *ortho*-methyl derivative **2a** with respect to the non-substituted amine **1a**. Due to the increased bulkiness of the aromatic ring, the monosubstituted BTBA is included from the *tert*-butyl side, which is located at the smaller edge of the host, while the phenyl ring resides near the secondary rim of the macrocycle.

Similar spectral results are obtained on investigating the behaviour of **2a** in the presence of γ-CD. The spectra (see the ESI†) recorded for solutions of the amine containing increasing amounts of the macrocycle reveal the same interactions for the *tert*-butyl group (with CD H3/H5/H6) already observed in the inclusion complex with β-CD. Conversely, the spectra do not report intermolecular correlation for the phenyl ring and the inner protons of the host, indicating a larger freedom of the aromatic ring in the complex, presumably due to the larger size of the cavity.

ROESY spectra of the sample containing amine **3a** and β-CD in an equimolar stoichiometric ratio show clear interactions both for *tert*-butyl and *ortho*-dimethyl substituents (see the ESI†). In particular the former is correlating with the inner H3/H5 and the primary rim (H6) protons and the latter show connections only with H3. In contrast, no intermolecular cross-peak has been recorded for phenyl ring.

Together these results suggest that the 2,6-disubstituted benzyl amine shows a mode of inclusion into β-CD similar to what was observed for monomethylated **2a**, however the lack of interactions of the aromatic proton with CD internal protons suggest a looser complex than that with **2a** in which the *tert*-butyl part of the amine is located close to the primary CD rim and the phenyl group of the guest exposed to the solvent from the secondary side of the host.

NOE considerations regarding the complex of **3a** with the larger cavity γ-CD are in line with the previous results exposed for the monosubstituted benzyl derivative (**2a**), that is less intense interactions with inner CD protons, but the same direction of inclusion (*tert*-butyl group inside the minor rim). Also in this case intermolecular NOEs are not observed for the aromatic proton of the amine.

An investigation on size increase of the guest *ortho*-substituent in the control of the inclusion direction is also described. Some ROESY spectra were measured for samples containing amine **6a** treated with 40–80% stoichiometric amounts of β-CD.

The presence of cross peaks (see the ESI†) connecting the methylene ring-substituents (of the ethyl group) of **6a** with H3 β-CD protons only, and which were not observed with H5 and H6, together with interactions of the *tert*-butyl portion with H3 (strong), H5 (medium) and H6 (weak), and connection of phenyl ring protons with H3, indicate that the inclusion of the amine into the CD occurs from the *tert*-butyl side.

By combining EPR and NMR data it was possible to conclude that the smaller association rate constants observed with **2b**–**3b** and **6b** described the inclusion process of the probe by the *tert*-butyl side.

## Nitroxide conformations

Information on the preferred conformations adopted by the different radicals in the various environments can be obtained from the magnitude of $a(H_\beta)$. The value of the hyperfine splitting constant for β-protons in alkyl nitroxides depends on the spin population in the $2p_\pi$-orbital of nitrogen ($\rho^\pi_N$) and on the dihedral angle ($\vartheta$) between the symmetry axis of this orbital and the N–C–$H_\beta$ plane (eqn (1)).[15]

$$a(H_\beta) = \rho_N^\pi \, (A_N + B_N \langle \cos^2 \vartheta \rangle) \quad (1)$$

The constant $A_N$ is small and usually neglected, while $B_N$ is *ca.* 59 G.[16] By using this value and by considering the splitting observed at the methyl protons in methyl benzyl nitroxide (13.34 G) where $\langle \cos^2 \vartheta \rangle = 0.5$ for symmetry reasons an approximate value of 0.45 for $\rho^\pi_N$ can be obtained.[8]

The knowledge of the approximate value of $\rho^\pi_N$ makes it possible to predict the preferred conformations adopted by the radicals both in solution and included inside the CD cavity. In conformation *A* (Scheme 4), where the dihedral angle between the Ar–C and N–O bonds ($\alpha$) is zero and ($\vartheta$) is for both hydrogens 30° the value of *a*(H) is expected to be *ca.* 19.9 G. In conformation *C*, $a(H_\beta)$ values equal to 19.9 G for one proton and $a(H_\beta) = 0$ G for the other proton are expected. However, a fast exchange between this conformation and the enantiomeric conformation *C** with $\alpha = -120°$ would make both hydrogens equivalent so that a value of *ca.* 10 G for both protons would be expected. In conformation *B*, $a(H_\beta)$ is expected to be about 6.0 G for both hydrogens.[17] If we restrict the analysis to the symmetric derivatives, the experimental values of $a(H_\beta)$ reported in Table 1 indicate that in water solution the minimum energy conformation of **1b** should be close to *C* while in nitroxides **3b** and **5b** the preferred conformation adopted should be very similar to *A*.

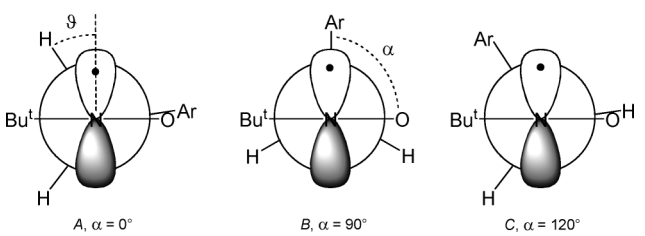


**Scheme 4**

When the probe **1b** is included inside the β-CD cavity, the radical is experiencing a less polar environment with respect to

water. This gives rise to a decrease of $\rho^{\pi}_{N}$ as indicated by the reduction observed both in the value of $a$(N) and $a(H_\beta)$. However, the inclusion of **1b** leads to a larger decrease in the value $a(H_\beta)$ (7.58 G) than expected based on eqn (1) (77% of the expected value of 9.62 G). This clearly suggests that a change in the conformation adopted by the radical is observed upon inclusion in the CD cavity and that the energy barrier between the two different conformations must be very low. The decrease in the hydrogen splitting implies that inside the CD cavity the conformation *B* in which the phenyl group is eclipsed by the N-2$p_\pi$ orbital is more important than in solution.

On the contrary, disubstituted derivatives **3b** and **5b** show a value of $a(H_\beta)$ (16.71 G and 15.63 G) much closer to that expected on the simple reduction of $\rho^{\pi}_{N}$ (97% and 95% of the expected values, respectively), this being an indication that the inclusion is not able to change drastically the occupancy of the minimum energy conformation. This behaviour is consistent with the assumption that the inclusion is occurring from the *tert*-butyl side, which is expected to leave the conformation around the benzylic bond similar to the one adopted in water.

In principle, the reduced differences in the values of $a(H_\beta)$ for the free and included species in **3b** and **5b** with respect to BTBN can also be related to a decrease in the conformational freedom around the $^{\bullet}ON–CH_2C_{Ar}$ bond deriving from an increase in the energy barrier for the bond rotation. Actually, in the presence of γ-CD, which forms in all cases host–guest complexes with the same geometry (*vide supra*), the inclusion of **1b** leads to a larger decrease in the value $a(H_\beta)$ (78% of the expected value) while with **3b** and **5b** the included radicals have $a(H_\beta)$ close to those expected from eqn (1) (92% and 95%, respectively).

In order to rationalize the result obtained in the presence of γ-CD, we performed a theoretical calculation of the rotational barrier of the $^{\bullet}ON–CH_2C_{Ar}$ bond in the derivatives **1b**, **3b** and **5b**. The barriers to internal rotation were calculated using the B3LYP/6-31+G(d,p) method.[18] The dependences of the potential energy on the dihedral angles (Fig. 3) were determined by scanning the dihedral angle from 0 to 360° with an increment of 20° and geometry optimization in each step. At each energy minimum, the molecular geometry was fully optimized.

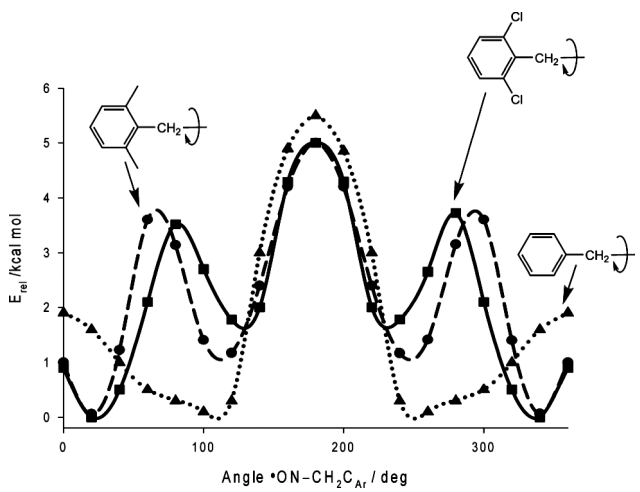


**Fig. 3** Relative energies as a function of the $^{\bullet}ON–CH_2C_{Ar}$ dihedral angle (α) in the nitroxides **1b**, **3b** and **5b**.

With **1b**, calculations indicated that conformations close to the geometry of *C* are the most stable as suggested by analysis of $a(H_\beta)$ splitting. Conformer *B* lies very close to conformer *C*, while conformer *A* is less stable than the conformer *C* by 2.0 kcal mol$^{-1}$. Analysis of the potential energy *vs*. dihedral angle plots (see Fig. 3) showed that the largest energy expenditures (5.5 kcal mol$^{-1}$) are required for the transformation between the two enantiomeric conformations *C* having $\alpha = \pm 120°$ and by passing with the phenyl and *tert*-butyl eclipsed.

On the contrary, with **3b** and **5b** calculations indicated that a conformation close to the geometry of *A* represents the most stable conformer. In this case conformer *C* is less stable than the conformers *A* by *ca.* 1.1 and 1.7 kcal mol$^{-1}$ in **3b** and **5b**, respectively. Analysis of the potential energy *vs*. dihedral angle plots (see Fig. 3) showed that a very large amount of energy (*ca.* 4 kcal mol$^{-1}$) is required for the $A \rightarrow C$ transformation. This confirms that **3b** and **5b** are indeed characterized by a reduced conformational freedom around the $^{\bullet}ON–CH_2C_{Ar}$ bond.

## Conclusions

Kinetic, and structural aspects of complexation by cyclodextrins play an essential role in the understanding of their functions and for the development of prospective applications. The solution structures are intimately related to molecular recognition, and the specific location of functional groups in the CD cavity, in particular in solution, may be a prerequisite for the construction of instructed chemical systems in which not only the equilibrium states but also the dynamic behaviour could be carefully controlled. By using specifically designed EPR spin probes and their corresponding diamagnetic precursors, we could distinguish different geometries of inclusion complexes. We also provided herein a data set for substituent effects on EPR parameters, association rate constants for complexation of nitroxides **2b–6b** by β- and γ-CD and the solution structures of the resulting complexes. Work to extend this approach to other supramolecular systems is in progress.

## Experimental

### General procedure for the preparation of amines 2a–6a

A toluene solution (150 ml) of *tert*-butyl-amine (15 mmols) and the appropriate substituted benzaldehyde (15 mmols), was stirred and heated under reflux for 10 h. During the reaction water was removed by a Dean–Stark apparatus. The solution was cooled and evaporated under reduced pressure to afford the corresponding imine (yield 90–95%). The imine (14 mmols) was then dissolved in a solution 1 : 1 of THF–methanol (150 ml), and stirred at room temperature for 2 h in the presence of $NaBH_4$ (14 mmols). Another portion of $NaBH_4$ was then added to the reaction mixture (14 mmols) and the solution was stirred further for 16 h. The solution was treated with HCl 6 N (150 ml) and the solvent was removed by evaporation under reduced pressure. The residue was treated with aqueous NaOH 5 N (100 ml) and extracted with $CH_2Cl_2$ (100 ml × 3). The organic phase was washed with water (100 ml), before being dried ($Na_2SO_4$) and evaporated under reduced pressure. The product was purified by column chromatography (eluent petroleum ether–ethyl acetate 6/4, v/v) to give the amine (yield 80–85%).

 

**2a.** Elemental analysis for $C_{12}H_{19}N$ Calc.: C, 81.30; H, 10.80; N, 7.90; Found C, 81.35; H, 10.72; N, 7.94; IR $\nu_{max}/cm^{-1}$ 3319 (NH), 748($C_{Ar}$-H); $^1$H-NMR (300 MHz, $CDCl_3$) $\delta$ 7.32–7.28 (m, 1H), 7.17–7.10 (m, 3H), 3.7 (s, 2H), 2.38 (s, 3H), 1.20 (s, 9H); GC-MS (*m*/*z*): 177 ($M^+$, 10) 162 ($M^+$–15, 33), 105 ($M^+$–72, 100); EPR parameters of the corresponding nitroxide **2b**: see Table 1.

**3a.** Elemental analysis for $C_{13}H_{21}N$ Calc.: C, 81.61; H, 11.06; N, 7.32; Found C, 81.70; H, 11.02; N, 7.42; IR $\nu_{max}/cm^{-1}$ 3322 (NH), 770 ($C_{Ar}$-H); $^1$H-NMR (300 MHz, $CDCl_3$) $\delta$ 7.12–6.93 (m, 3H), 3.74 (s, 2H), 2.41 (s, 6H), 1.19 (s, 9H); GC-MS (*m*/*z*): 191 ($M^+$, 10) 176 ($M^+$–15, 25), 119 ($M^+$–72, 100); EPR parameters of the corresponding nitroxide **3b**: see Table 1.

**4a.** Elemental analysis for $C_{11}H_{16}ClN$ Calc.: C, 66.83; H, 8.16; Cl, 17.93; N, 7.08; Found C, 66.91; H, 8.22; Cl, 17.68; N, 7.04; IR $\nu_{max}/cm^{-1}$ 3313 (NH), 1055 ($C_{Ar}$-Cl), 758 ($C_{Ar}$-H); $^1$H NMR (300 MHz, $CDCl_3$) $\delta$ 7.46 (dd, 1H, $J$ = 7.4 and 1.5 Hz), 7.31 (dd, 1H, $J$ = 7.4 and 1.5 Hz), 7.20–7.15 (m, 2H), 3.81 (s, 2H), 1.19 (s, 9H); GC-MS (*m*/*z*): 197 ($M^+$, 5) 182 ($M^+$–15, 60), 125 ($M^+$–72, 100); EPR parameters of the corresponding nitroxide **4b**: see Table 1.

**5a.** Elemental analysis for $C_{11}H_{15}Cl_2N$ Calc.: C, 56.91; H, 6.51; Cl, 30.54; N, 6.03; Found C, 56.55; H, 6.62; Cl, 30.25; N, 5.94; IR $\nu_{max}/cm^{-1}$ 3321 (NH), 1058 ($C_{Ar}$-Cl), 768 ($C_{Ar}$-H); $^1$H-NMR (300 MHz, $CDCl_3$) $\delta$ 7.28 (d, 2H, $J$ = 8.4 Hz), 7.11 (t, 1H, $J$ = 8.4 Hz), 4.00 (s, 2H), 1.18 (s, 9H); GC-MS (*m*/*z*): 231 ($M^+$, 2) 216 ($M^+$–15, 80), 159 ($M^+$–72, 100); EPR parameters of the corresponding nitroxide **5b**: see Table 1.

**6a.** Elemental analysis for $C_{13}H_{21}N$ Calc.: C, 81.61; H, 11.06; N, 7.32; Found C, 81.72; H, 11.01; N, 7.26; IR $\nu_{max}/cm^{-1}$ 3319 (NH), 758 ($C_{Ar}$-H); $^1$H-NMR (300 MHz, $CDCl_3$) $\delta$ = 7.34–7.32 (m, 1H), 7.21–7.15 (m, 3H), 3.74 (s, 2H), 2.74 (q, 2H, $J$ = 7.5 Hz), 1.26 (t, 3H, $J$ = 7.5 Hz), 1.20 (s, 9H); GC-MS (*m*/*z*): 191 ($M^+$, 10) 176 ($M^+$–15, 45), 119 ($M^+$–72, 100); EPR parameters of the corresponding nitroxide **6b**: see Table 1.

## Notes and references


1 A. Harada, *Acc. Chem. Res.*, 2001, **34**, 456.
2 H.-R. Tseng, S. A. Vignon and J. F. Stoddart, *Angew. Chem., Int. Ed.*, 2003, **42**, 1491.
3 W. H. Chen, M. Fukudome, D. Q. Yuan, T. Fujioka, K. Mihashi and K. Fujita, *Chem. Commun.*, 2000, 541; T. Felder and C. A. Schalley, *Angew. Chem., Int. Ed.*, 2003, **42**, 2258; H. Onagi, C. J. Blake, C. J. Easton and S. F. Lincoln, *Chem.–Eur. J.*, 2003, **9**, 5978.
4 Themed issue Jean-Pierre Sauvage, *Chem. Soc. Rev.*, 2009, 38, pp. 1509–1824.
5 Z. Zhong, A. Ikeda and S. Shinkai, *J. Am. Chem. Soc.*, 1999, **121**, 11906; A. Arduini, R. Ferdani, A. Pochini, A. Secchi and A. Ugozzoli, *Angew. Chem., Int. Ed.*, 2000, **39**, 3453; T. Yamagishi, A. Kawahara, J. Kita, M. Hoshima, A. Umehara, S. Ishida and Y. Nakamoto, *Macromolecules*, 2001, **34**, 6565; A Credi, S. Dumas, S. Silvi, M. Venturi, A. Arduini, A. Pochini and A. Secchi, *J. Org. Chem.*, 2004, **69**, 5881; A. Arduini, F. Ciesa, M. Fragassi, A. Pochini and A. Secchi, *Angew. Chem., Int. Ed.*, 2005, **44**, 278; A. Arduini, R. Bussolati, A. Credi, A. Pochini, A. Secchi, S. Silvi and M. Venturi, *Tetrahedron*, 2008, **64**, 8279; A. Arduini, R. Bussolati, A. Credi, G. Faimani, S. Garaudèe, A. Pochini, A. Secchi, M. Semeraro, S. Silvi and M. Venturi, *Chem.–Eur. J.*, 2009, **15**, 3230.
6 J. Pozuelo, F. Mendicuti and W. L. Mattice, *Macromolecules*, 1997, **30**, 3685; J. E. H. Buston, J. R. Young and H. L. Anderson, *Chem. Commun.*, 2000, 905; K. Miyake, S. Yasuda, A. Harada, J. Sumaoka, M. Komiyama and H. Shigekawa, *J. Am. Chem. Soc.*, 2003, **125**, 5080; J. W. Park and H. Song, *Org. Lett.*, 2004, **26**, 4869.
7 T. Oshikiri, Y. Takashima, H. Yamaguchi and A. Harada, *J. Am. Chem. Soc.*, 2005, **127**, 12186; T. Oshikiri, Y. Takashima, H. Yamaguchi and A. Harada, *Chem.–Eur. J.*, 2007, **13**, 7091.
8 M. Lucarini, B. Luppi, G. F. Pedulli and B. P. Roberts, *Chem.–Eur. J.*, 1999, **5**, 2048.
9 P. Franchi, M. Lucarini, E. Mezzina and G. F. Pedulli, *J. Am. Chem. Soc.*, 2004, **126**, 4343; P Franchi, G. F. Pedulli and M. Lucarini, *J. Phys. Chem. A*, 2008, **112**, 8706; E. Mileo, P. Franchi, R. Gotti, C. Bendazzoli, E. Mezzina and M. Lucarini, *Chem. Commun.*, 2008, 1311.
10 M. Lucarini, P. Franchi, G. F. Pedulli, C. Gentilini, S. Polizzi, P. Pengo, P. Scrimin and L. Pasquato, *J. Am. Chem. Soc.*, 2005, **127**, 16384.
11 (*a*) Y. Kotake and E. G. Janzen, *J. Am. Chem. Soc.*, 1988, **110**, 3699; Y Kotake and E. G. Janzen, *Chem. Phys. Lett.*, 1988, **150**, 199; Y. Kotake and E. G. Janzen, *Chem. Express*, 1988, **3**, 715; Y. Kotake and E. G. Janzen, *J. Am. Chem. Soc.*, 1989, **111**, 2066; Y. Kotake and E. G. Janzen, *J. Am. Chem. Soc.*, 1989, **111**, 5138; Y. Kotake and E. G. Janzen, *Free Rad. Res. Comms.*, 1990, **10**, 103.
12 X. Zhang, G. Gramlich, X. Wang and W. M. Nau, *J. Am. Chem. Soc.*, 2002, **124**, 254.
13 T. Kida, Y. Fujino, K. Miyawaki, E. Kato and M. Akashi, *Org. Lett.*, 2009, **11**, 5282.
14 M. Lucarini, E. Mezzina and G. F. Pedulli, *Eur. J. Org. Chem.*, 2000, 3927.
15 C. Heller and H. M. McConnell, *J. Chem. Phys.*, 1960, **32**, 1535.
16 H. G. Aurich, *"The Chemistry of Amino, Nitroso, Nitro Compounds and of their Derivatives"*, (Ed.: S. Patai), Wiley, Chichester, 1982, p. 565.
17 Of course, it must be borne in mind that predictions based on eqn (1) will be only semi-quantitative and that the conformations indicated are averages over the populated torsional states.
18 M. J. Frisch, G. W. Trucks, H. B. Schlegel, G. E. Scuseria, M. A. Robb,J. R. Cheeseman, J. A. Montgomery, T. Vreven, K. N. Kudin, J. C. Burant, J. M. Millam, S. S. Iyengar, J. Tomasi, V. Barone, B. Mennucci, M. Cossi, G. Scalmani, N. Rega, G. A. Petersson, H. Nakatsuji, M. Hada, M. Ehara, K. Topyota, R. Fukuda, J. Hasegawa, M. Ishida, T. Makajima, Y. Honda, O. Kitao, H. Nakai, M. Klene, X. Li, J. E. Know, H. P. Hratchian, J. B. Cross, V. Bakken, C. Adamo, J. Jaramillo, R. Gomperts, R. E. Stratmann, O. Yazyev, A. J. Austlin, R. Cammi, C. Pomelli, J. W. Ochterski, P. Y. Ayala, K. Morokuma, G. A. Voth, P. Salvador, J. J. Dannenberg, V. G. Zakrzewski, S. Dapprich, A. D. Daniels, M. C. Strain, O. Farkas, D. K. Malick, A. D. Rabuck, K. Raghavachari, J. B. Foresman, J. V. Ortiz, Q. Cui, A. G. Baboul, S. Cliffors, J. Cioslowski, B. B. Stefanov,G. Liu, A. Liashenko, P. Piskorz, I. Komaromi,R. L. Martin,D. J. Fox, T. Keith, M. A. Al-Latham, C. Y. Peng, A. Nanayakkara, M. Challacombe, P. M. W. Gill, B. Johnson, W. Chen, M. W. Wong, C. Gonzalez and J. A. Pople, *Gaussian 03*, Revision B05, Gaussian, Inc., Pittsburgh, 2003.